ENVIRONMENTAL RESEARCH
LETTERS

LETTER • OPEN ACCESS

Climate change impacts on the energy system: a model comparison

To cite this article: Victhalia Zapata *et al* 2022 *Environ. Res. Lett.* **17** 034036

ENVIRONMENTAL RESEARCH
LETTERS

OPEN ACCESS

RECEIVED
27 December 2020

REVISED
20 January 2022

ACCEPTED FOR PUBLICATION
2 February 2022

PUBLISHED
28 February 2022

LETTER

Climate change impacts on the energy system: a model comparison

Victhalia Zapata[1], David E H J Gernaat[1,2], Seleshi G Yalew[3], Silvia R Santos da Silva[4,5,6], Gokul Iyer[5], Mohamad Hejazi[5,7] and Detlef P van Vuuren[1,2]

[1] Copernicus Institute of Sustainable Development, Utrecht University, Utrecht, The Netherlands
[2] PBL The Netherlands Environmental Assessment Agency, The Hague, The Netherlands
[3] Department of Land & Water Management, IHE-Delft Institute for Water Education, Delft, The Netherlands
[4] Department of Atmospheric and Oceanic Science, University of Maryland, College Park, MD, United States of America
[5] Joint Global Change Research Institute, Pacific Northwest National Laboratory, College Park, MD, United States of America
[6] College of Science, George Mason University, Fairfax, VA, United States of America
[7] King Abdullah Petroleum Studies and Research Center (KAPSARC), Riyadh, Saudi Arabia

E-mail: v.h.zapatacastillo@uu.nl

Keywords: climate impacts, energy systems, renewable energies, energy models, RCP2.6, RCP6.0, SSP2

Abstract

Increasing renewable energy use is an essential strategy for mitigating climate change. Nevertheless, the sensitivity of renewable energy to climatic conditions means that the energy system's vulnerability to climate change can also become larger. In this research, we used two integrated assessment models and data from four climate models to analyse climate change impacts on primary energy use at a global and regional scale under a low-level (RCP2.6) and a medium-level (RCP6.0) climate change scenario. The impacts are analysed on the energy system focusing on four renewable sources (wind, solar, hydropower, and biomass). Globally, small climate impacts on renewable primary energy use are found in both models (5% for RCP2.6 and 6% for RCP6.0). These impacts lead to a decrease in the use of fossil sources for most regions, especially for North America and Europe under the RCP60 scenario. Overall, IMAGE and GCAM provide a similar signal impact response for most regions. E.g. in Asia (excluding China and India), climate change induces an increase in wind and hydropower use under the RCP6.0 scenarios; however, for India, a decrease in solar energy use can be expected under both scenarios and models.

1. Introduction

The energy sector is well known as a major cause of climate change, accounting for about two-thirds of CO_2 emissions worldwide in 2018 [1]. At the same time, the sector is also impacted by climate change on both supply and demand of energy [2, 3]. The vulnerability of the energy system to climate change could increase in the future, given the expected increasing role of renewable energy use. Bioenergy, hydropower, solar, and wind power are all sensitive to climatic conditions. For example, hydropower supply may be affected by long-term changes in streamflow. Cloudiness, temperature, wind speed, CO_2 fertilisation and precipitation affect the energy potential of solar, wind, and bioenergy [2–4]. Previous literature reviews on this topic conclude that there is a need for further comprehensive knowledge about climate change impacts on the energy system as a whole and on a global scale [2, 3]. Such an assessment should also address the uncertainty in how climate change would evolve and the ability of the energy system to adapt to such impacts. While two prior studies have investigated climate system impacts using a single modelling system [5, 6], our study goes beyond them by implementing a two-model inter-comparison with a systematic approach for analysing the uncertainty in climate impacts on the primary renewable energy generation at a global scale. It considers system interactions on a range of energy sources and technologies and the impacts under two scenarios with a low level and a medium level of climate change (RCP2.6 and RCP6.0, respectively). The analysis is performed using climate projections from four general circulation models (GCMs) and two integrated assessment models (IAMs). The GCMs are: GFDL-ESM2M,

HADGEM2-ES, IPSL-CM5A-LR, and MIROC5 [7]; and the IAMs are IMAGE [8], and GCAM [9]. IAMs are global models that analyse diverse and complex interactions between human activities, including the energy and earth systems. These models are used, for example, to develop scenarios with and without climate policy and to analyse the consequent implications for key systems, such as energy or land. For the analysis here, the information of climate change impacts on the energy potential and costs of eight renewable energy technologies from Gernaat *et al* [5] are implemented as input data (in the form of cost–supply curves) in the IAM models.

2. Methodology

2.1. Overall methodology

We first account for climate change impacts on the renewable energy potential and generation costs using the dataset produced in Gernaat *et al* [5]. The impacts on energy potential are based on the results of four GCMs from the ISIMIP2b database [7] under two representative concentration pathways (RCPs): RCP6.0 and RCP2.6. The RCP6.0 is considered a reference scenario; it leads to a temperature rise in the range of about 2.5 °C–4.5 °C by 2100. The RCP2.6 aims to keep global warming below 2 °C by 2100, consistent with the goal of the Paris Agreement [7] (temperature projections from each GCM are shown in appendices). In the Gernaat *et al* [5] study, renewable energy potential maps for the most developed and commercially available technologies were built; they are utility-scale photovoltaic (PV), rooftop PV and concentrating solar power (CSP) for solar sources; offshore and onshore wind; hydropower, and first- and second-generation bioenergy potential. The climate data from the ISIMIP2b database was used to obtain climate change's impact on these renewable energy potentials at the grid level (0.5° × 0.5°) using geographical and technical constraints, such as excluding natural reserves and forest areas [5]. To compute the solar potentials, solar irradiance, air temperature, and wind speed data were used. For computing the wind potentials, wind speed data was used. The hydropower potential depends on run-off data, and the bioenergy potentials depend on sugar, maise and lignocellulosic yields with CO_2 fertilisation. The yields and run-off data were generated using the LPJmL model, following the ISIMIP2b protocol with GCMs data [7]. The generation costs (namely, the economic potential) was made based on the interest rate, capital costs and learning rates [10–12]. Impacts on renewable energy potentials were calculated for three time periods: the historical 1970–2000 period (using historical climate data) and projections for 2031–2070 and 2071–2100. In our study, we combined these technical and economic potential maps to obtain cost–supply curves. They provide information on the generation costs of a unit of energy potential consumed and are obtained by sorting the grid cells corresponding to each IAMs region division.

The information on changes in cost–supply curves was used to calculate climate impacts on future primary energy use using IMAGE [13] and GCAM [14] models. For comparison purposes, the IAMs results are aggregated into ten macro-regions (as described in appendix F). The comparison is not straightforward as the climate impacts depend on the dynamics between energy potential and cost and on indirect impacts (i.e. the impacts in one source resulting from system compensation for the changes in the supply levels of other sources). Concerning impacts on fossil energy use, only indirect impacts were analysed. Note that there could be climate impacts on the cooling system of thermal power plants that are not included in this analysis [15].

The IAM models were run using assumptions on the energy system consistent with the climate scenario assumed (i.e. no new climate policy for the RCP6.0 scenario and strong climate policy for the RCP2.6 scenario). The analysis thus covers uncertainty in the energy system response (across IAMs), the level of climate change (across scenarios), and the climate system uncertainty (across GCMs).

2.2. Scenarios description

The two IAMs run a scenario based on the SSP2 pathway [16]. SSP2 is a 'middle of the road' pathway, i.e. the world follows a path with medium assumptions for future socio-economic and technological development [17]. The SSP2 baseline scenario (no new climate policy) is combined with the RCP6.0 climate data, following an expected climate outcome (SSP2-RCP6.0-CI, see table 1). The IAM models also run a climate policy scenario that used a carbon tax for reducing emissions consistent with the objective of the Paris Agreement to keep temperature rise well below 2 °C. This scenario was combined with the RCP2.6 climate data (SSP2-RCP2.6-CI). As a reference, two scenarios were implemented without climate impacts using a constant ISIMIP2b historical climate data (SSP2-RCP6.0-NoCI and SSP2-RCP2.6-NoCI). Finally, a last set of scenarios are used to assess direct climate impact on two separate sources: biomass and wind. The scenarios previously described were implemented using climate modelled data from four GCMs: GFDL-ESM2M, HADGEM2-ES, IPSL-CM5A-LR, and MIROC5 [7].

2.3. Impact on renewable energy potential

Figure 1 shows climate impacts on renewable energy potentials aggregated from grid cell level to macro and global scales under the RCP2.6 and RCP6.0 scenarios for the period 2071–2100 (as calculated by Gernaat *et al* [5]). On the global scale, the most pronounced climate impacts are found for the biomass potential under both scenarios (with a higher increase in potential under the RCP6.0). Note that

Table 1. Scenarios implemented.

		Climate data	
		Without climate change impact	With climate change impact
Socioeconomic development	SSP2-RCP6.0	SSP2-RCP6.0-NoCI	SSP2-RCP6.0-CI
	SSP2-RCP2.6	SSP2-RCP2.6-NoCI	SSP2-RCP2.6-CI
Sensitivity runs	Biomass only	SSP2-RCP6.0-NoCI	SSP2-RCP6.0-Bio-CI
	Wind only	SSP2-RCP6.0-NoCI	SSP2-RCP6.0-Wind-CI

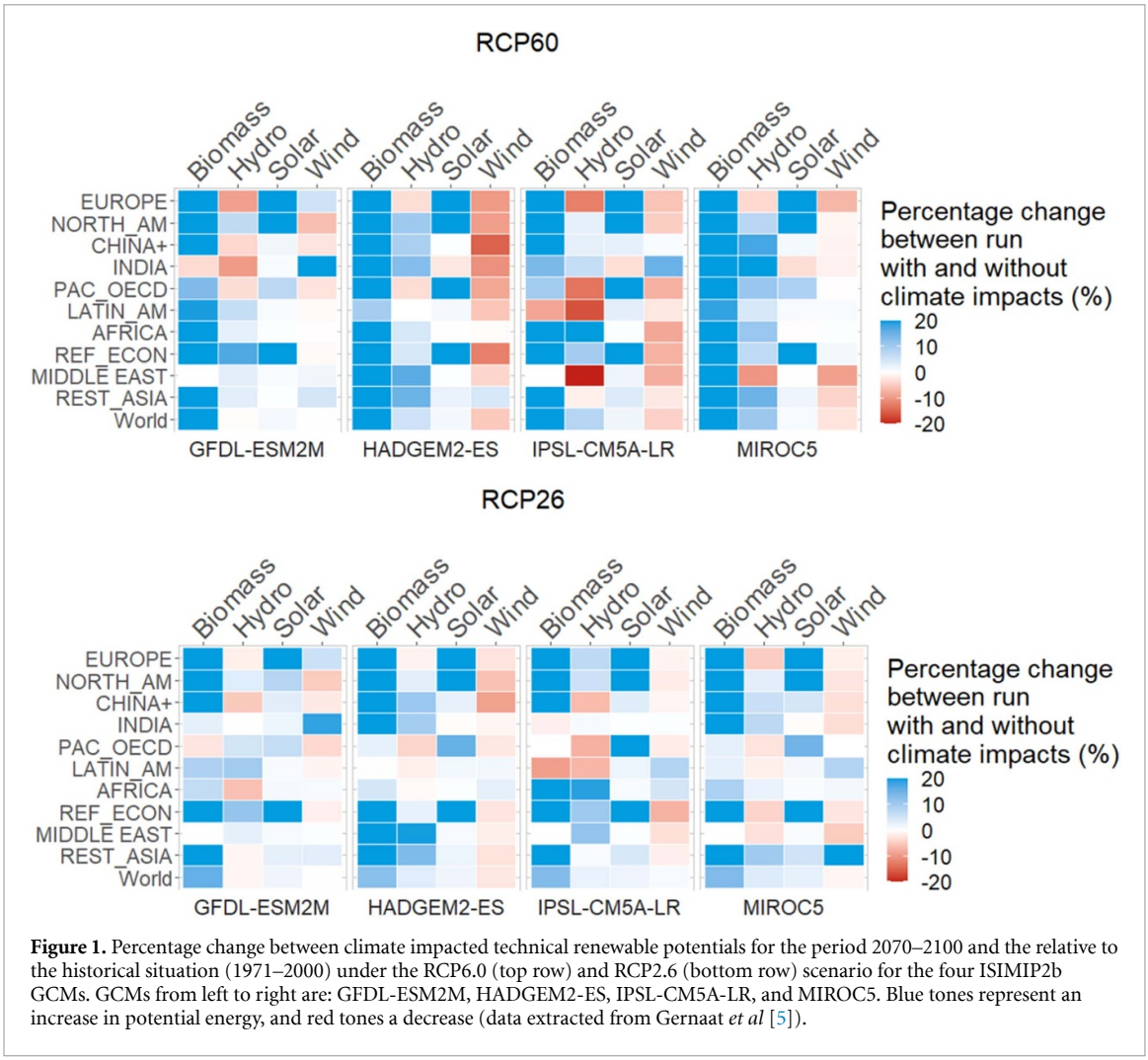

Figure 1. Percentage change between climate impacted technical renewable potentials for the period 2070–2100 and the relative to the historical situation (1971–2000) under the RCP6.0 (top row) and RCP2.6 (bottom row) scenario for the four ISIMIP2b GCMs. GCMs from left to right are: GFDL-ESM2M, HADGEM2-ES, IPSL-CM5A-LR, and MIROC5. Blue tones represent an increase in potential energy, and red tones a decrease (data extracted from Gernaat *et al* [5]).

our method accounts for the CO_2 fertilisation effect on crop yields. I.e. the increase in crop yields that results from increased levels of CO_2 in the atmosphere. Although this effect has been demonstrated by experiments and satellite imaging in the last years [5], there is still high uncertainty concerning its potential implications given the large range of results from distinct crop models [18]. The Gernaat *et al* [5] study analyses this effect. He shows that without the influence of the CO_2 fertilisation effect, possible positive climate impacts on yields can be considerably less pronounced (under the RCP6.0 scenario); while the negative impacts on yields can be larger, like in Sub-Saharan Africa and Mexico.

Regarding solar energy potential, the expected impacts are mostly positive at the macro-regions aggregated level. However, the impacts are more varied at higher spatial resolution, depending on the local changes in temperature, wind speed, and irradiance [5]. Overall, impacts on wind energy potential are mostly negative due to lower wind speed. It should be noted that there is considerable variation in the climate impacts on energy potential across the different climate models. This can be illustrated with Latin America for Biomass and hydropower, where there is no consensus on the direction of response to climate. Hence, the impact on the energy system is analysed for each GCM dataset separately.

2.4. Integrated assessment models

The IMAGE and GCAM models are used to calculate climate impacts on primary energy use. Both IAMs

analyse the interaction between human and natural systems with a global and long-term scope [19]. In IMAGE, the world is divided into 26 regions with an annual time step [5, 13], while in GCAM, the world is divided into 32 regions with a 5 year time-step [6, 14]. These models represent the energy system from the extraction of primary resources until the transformation processes that produce the final energy carriers, using comprehensive technology databases. Both IAMs use IEA energy balances [20] for the calibration of energy flows. Capital costs and conversion efficiencies per energy source for the two models are described in [21]. In both IAMs, resource-cost supply curves affect the calculation of each technology's levelized cost (LC), which has implications for the models' investment decisions. In the IAMs, each technology competes for a share of investment based on technology costs modelled through a logit function. The overall methodology presents similarities for both IAMs. However, there are also some differences in the cost calculation that can affect decisions on which technology gains a larger market share, and they could impact which primary energy source is used more. For the power sector, the LC equation for IMAGE is explained in [22] and for GCAM in [6]. In both models, the LC is calculated as a function of the capital costs, a fixed charge rate (covering for instance the annualised interest during construction), the operation and maintenance costs and, if relevant, the annual fuel costs (for bioenergy), annual carbon storage costs, backup costs for system flexibility, and impact of system integration on actual load factors. The generation costs from the cost curves looked at in this paper directly affect the levelized costs in both models.It should be noted that for GCAM, the costs are calculated using a fixed exogenously defined capacity factor of technologies; it represents electricity supply on an annual mean basis. However, in IMAGE, electricity generation is calculated using residual load duration curves (RLDCs) divided into load bands. It should also be noted that GCAM represents renewable intermittency in the form of cost that vary with the share of intermittent renewables in the grid and add to the LC in the case of solar and wind [21]. For GCAM, cost supply curves are implemented for wind onshore and solar sources since bioenergy and hydropower do not rely on supply curves in this model. Still, the input data of technical potential is used for hydropower and bioenergy (further information in appendix A).

3. Results

3.1. Climate change impact on the energy system

3.1.1. SSP2-RCP6.0 scenario

Climate impact on the energy system under the SSP2 baseline scenario for the period 2071–2100 is illustrated in figure 2 (further results for the period 2031–2070 and under the SSP1 scenario in appendix D). The four graphs from each GCM show the mean (over time and IAMs subregion) percentage change of primary energy use between the scenario with (SSP2-RCP6.0-CI) and without climate impact (SSP2-RCP6.0-NoCI) for the IAMs considered. An increase in primary energy use by climate impact is defined as a positive impact shown with blue colour tones. A decrease is defined as a negative impact shown with red colour tones. Under this scenario, IMAGE and GCAM depict a similar impact on the use of different energy sources, ranging from −20% to 20% change in primary energy use between the scenarios with and without climate impacts in the ten macro-regions. Significant impacts are projected for bioenergy use from both IAMs but with higher impacts from IMAGE results, especially for North America, Africa and Europe (further analysis on these differences in section 3.2). The input data of bioenergy potential shows an increase due to CO_2 fertilisation (figure 1), which leads to increased use of bioenergy in both IAMs results in all regions except for India and the Middle East for IMAGE, where the cost (from the cost–supply curves) is higher in the RCP6.0 scenario. For the other sources, there are more differences between the IAMs results.

The largest variation between the IAMs response to climate impacts across the GCMs runs is for solar energy (also for the period 2031–2070 in appendix D), especially for North America and the Reforming Economies. GCAM shows a decrease in solar use for most regions caused by compensation for the increased use of the other renewables (mainly biomass). However, IMAGE shows mostly an increase caused by the impacts on solar potential. The differences here are related to different implementation of the cost–supply curves (as explained in section 2) and system compensation, i.e. differences in how an increase in one source is compensated by a decrease in other sources. Furthermore, the outcome variations can also be driven by differences in technological and economic assumptions between the IAMs (shown in appendix B), such as assumptions on the learning rate of energy technologies and system costs. They all affect the LCs of energy sources, which influences the priority given to each energy technology.

Overall, the IAMs show an increase in renewables use for all regions, with the global average of 6% (with 17.6% of standard deviation) across all IAMs and GCMs. However, for specific source-region combinations, the climate impacts can be negative. For example, the Pacific OECD region has the largest reduction in the use of wind according to both IAMs, resulting from a reduction in wind potential (figure 1). Further, a significant reduction in hydropower use is shown by both IAMs for this region (across GFDL-ESM2M and IPSL-CM5A-LR) by decreased hydropower potential. Consistent results across all IAMs and GCMs are found for Rest

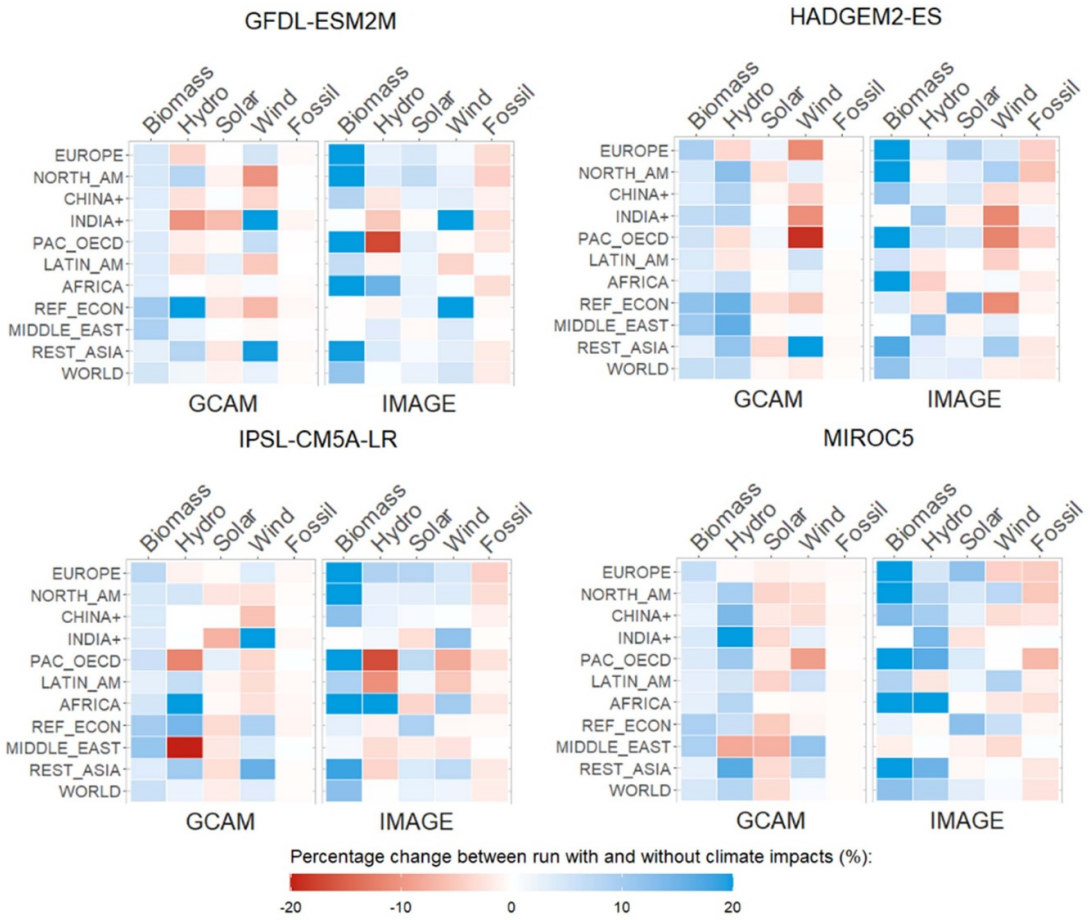

Figure 2. Changes in primary energy use under the SSP2-RCP6.0 scenario between the runs with and without climate change impacts for the period 2071–2100. Impacts are compared between IMAGE and GCAM for each GCM (top left: GFDL-ESM2M, top right: HADGEM2-ES, bottom left: IPSL-CM5A-LR, and bottom right: MIROC5). Blue tones represent positive impacts and red tones negative impacts by climate change.

Asia and India. For Rest Asia, an increase in hydropower (5% from IMAGE and 12% from GCAM) and wind energy use is denoted (5% from IMAGE and 16% from GCAM). For India, a decrease in solar energy use is denoted (2% from IMAGE and 4% from GCAM). Additionally, for China, the aggregated impacts on renewables use are positive, mainly by increased bioenergy (11% from IMAGE and 4% from GCAM) and hydropower use (3% from IMAGE and 5% from GCAM). However, a consistent decrease in its wind use is noted (1% from IMAGE and 4% from GCAM).

Concerning fossil sources, the results correspond to indirect impacts. Globally and for all regions, a reduction in its use is expected from both IAMs (global average of 2% from IMAGE and 0.3% from GCAM) for compensating the increase in renewables use, especially bioenergy. Only for India and based on HADGEM2-ES result, a small increase is reported for compensating the decrease in wind use. In contrast, the largest decrease in fossil use can be expected for North America (5% from IMAGE and 0.2% from GCAM) and Europe (4% from IMAGE and 0.5% from GCAM) consistently across all IAMs and GCM results.

3.1.2. SSP2-RCP2.6 scenario

Climate impacts under the SSP2-RCP2.6 scenario for the period 2071–2100 is illustrated in figure 3. Since this is a mitigation scenario, there is a larger reliance on renewable energy technologies to reduce energy-sector greenhouse gas emissions, potentially making the energy system more vulnerable to climate change. In this regard, negative impacts on the aggregated renewables use can be expected for Middle East (based on IMAGE), Latin America and Pacific OECD region (based on GCAM), while in the SSP2-RCP60 scenario, the impacts are on average positive for all regions. However, aggregated across all sources and at the global scale, our results do not signal a detrimental effect on the use of renewables as we have found an average increase in the primary renewable energy consumption of 5.2% (±24.2%) for the SSP2-RCP2.6 scenario and considering both IAMs.

Under this scenario, more variations in the signal response are found between the IAMs and GCMs

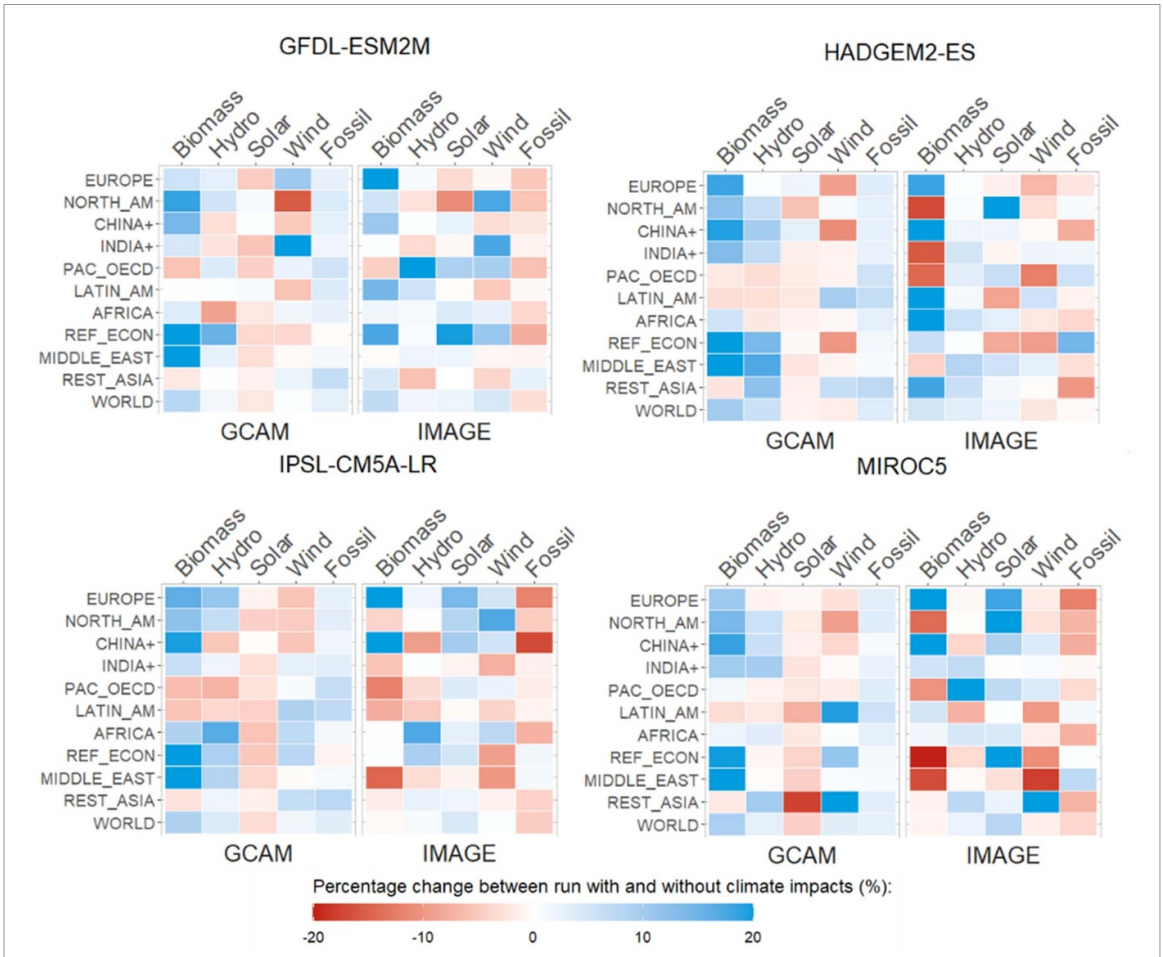

Figure 3. Changes in primary energy use under the SSP2-RCP2.6 scenario between the runs with and without climate change impacts for the period 2071–2100. Impacts are compared between IMAGE and GCAM for each GCM (top left: GFDL-ESM2M, top right: HADGEM2-ES, bottom left: IPSL-CM5A-LR, and bottom right: MIROC5). Blue tones represent positive impacts and red tones negative impacts by climate change.

for all renewables with solar energy use depicting the largest variability across the IAMs results. Especially for the Pacific OECD region, North America, and Africa, GCAM and IMAGE show different signal results. For bioenergy use, the variability between the IAMs results is also higher than under the SSP2-RCP6.0 scenario. The variation is the largest for the Middle East, where the IAMs results have opposite signals. Note that for this source, the expected impacts are on average lower than in the RCP6.0 case, as the CO_2 fertilisation effect is also lower. E.g. for Pacific OECD, a consistent bioenergy decrease by climate impacts is expected under this mitigation scenario, while an increase can be expected under the SSP2-RCP6.0 scenario.

A consistent result across the IAMs and most GCMs is the expected decrease in bioenergy use in the Pacific OECD region due to decreased energy potential (for GFDL-ESM2M and IPSL-CM5A-LR models) and increased generation costs for HADGEM2-ES. Further, a consistent bioenergy use increase can be expected for Europe (20% from IMAGE and 13% from GCAM), Africa (6% from IMAGE and 5% from GCAM), and China (18% from both IAMs) due to positive climate impacts in bioenergy potential (also for 2031–2070 as shown in appendix D). For Rest Asia, an increase in hydropower use can be expected (3% from IMAGE and 6% from GCAM) due to a projected increase in water run-off. Additionally, for India, a consistent decrease in solar energy use is observed (−3% from GCAM and −1% from IMAGE) by lower solar potentials.

3.2. Direct climate change impact on energy sources

In this section, direct climate impacts on wind and bioenergy are analysed (further analysis in appendix D). To this end, input data of energy potential and cost supply curves with climate impact are implemented on one source per run. In contrast, for the other sources, input data is based on historical climate values. This enables to exclude indirect impacts related to system interactions.

Figure 4 shows the direct climate impact on wind energy use for the period 2071–2100. In nearly all cases, the results directly reflect the changes in technical potential (figure 1), but there are some exceptions. For example, the results in Rest Asia and the

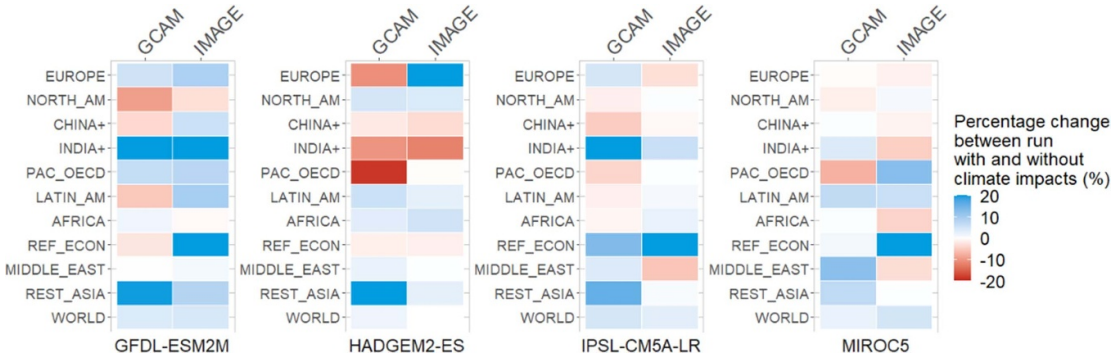

Figure 4. Climate impact direct effect on wind primary energy generation under the SSP2-RCP6.0 scenario for the period 2071–2100. The graphs correspond to the percentage change of wind use with and without climate impact for GCAM and IMAGE for the four GCMs (GFDL-ESM2M, HADGEM2-ES, IPSL-CM5A-LR, and MIROC5). Blue tones represent positive impacts and red tones negative impacts by climate change.

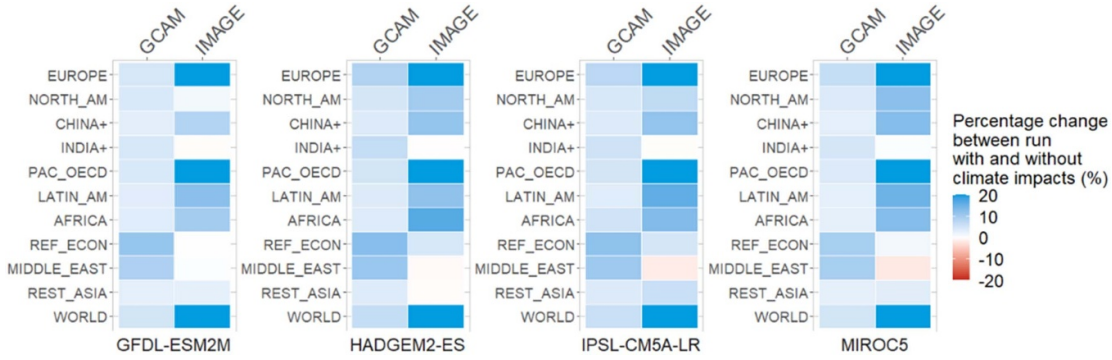

Figure 5. Climate impact direct effect on biomass primary energy generation under the SSP2-RCP6.0 scenario for the period 2071–2100. The graphs correspond to the percentage change of wind use with and without climate impact for GCAM and IMAGE and the four GCMs (GFDL-ESM2M, HADGEM2-ES IPSL-CM5A-LR, and MIROC5). Blue tones represent positive impacts and red tones negative impacts by climate change.

Reforming Economies (both IAMs for IPSL-CM5A-LR) show an increase in wind use despite negative climate impacts at the overall potential level. The main cause is that within the supply-costs curve, some parts experience cost reduction. Furthermore, different impacts between GCAM and IMAGE can be observed in some cases, such as in Europe and the Middle East. There are three main reasons for these differences. First, IMAGE implements climate impacts on both wind onshore and offshore, while in GCAM, the analysis is done considering only wind onshore. Second, IMAGE implements an inter-region learning parameter (not implemented by GCAM) where a reduction in cost from one region affects the cost of other regions. Finally, differences in modelling the investment decisions between the IAMs, as explained in the methods.

Figure 5 shows direct climate impacts on bioenergy use. Both IAMs show an increase in biomass use with larger expected impacts from IMAGE results. Differences in sensitivity to impacts in bioenergy potential are related to differences in the implementation of the input data (GCAM uses the overall potential to scale underlying cost curves). Furthermore, capital cost and variable cost assumptions for bioenergy technologies are lower in IMAGE than in GCAM.

On average for the world, it can be expected an increase in bioenergy use of 8% $\pm$ 7% due to climate impacts on technical potential when considering the effect of CO_2 fertilisation on crops (figure 1). India and Middle East regions have the lowest positive impact on bioenergy use due to low impacts on their average bioenergy potential (GFDL-ESM2M and IPSL-CM5A-LR) or higher cost (implemented only by IMAGE) for second-generation bioenergy (HADGEM2-ES, MIROC5). In contrast, the largest direct impact on bioenergy use can be expected for Africa, PAC_OECD and Europe regions.

4. Conclusions and discussion

In this research, we looked at the impacts of climate change on primary energy use, considering both climate model and energy model uncertainty. This analysis was done under a low level (SSP2-RCP2.6) and a medium level (SSP2-RCP6.0) climate change scenarios and focused on the 2071–2100 period. The

climate model uncertainty is well reflected in the outcome variations for direct impacts on renewables and the energy system response, as shown by the differences between the IMAGE and GCAM results. While the impacts correlate with those in the overall potential for most cases, this is not always true. The key reasons are that changes in the cost–supply curve may differ from the changes in the overall potential, and underlying model dynamics. Altogether, several significant findings can be made.

First, the two IAM models provide a similar signal response to climate change impacts for most regions and energy sources. However, outcome variation between the IAMs across the GCMs is large for solar energy use under both scenarios. Differences between the IAMs are determined by differences in modelling power investment decisions and technological and economic assumptions. Such as assumptions for the learning rate of energy technologies, system costs as capital costs, lifetime operation of powerplants, and inter-regional learning transference assumptions in which a reduction in cost from one region affects the cost on other regions.

The results show that climate change, under the SSP2-RCP6.0 scenario, could increase bioenergy use for all regions due to the positive impact of the CO_2 fertilisation effect on yields, as shown in earlier studies [5]. Other robust findings across the models are the increase in hydropower and wind energy use for Rest Asia, the decrease in solar use for India and the increase in hydropower use for China. Furthermore, despite climate impacts, fossil energy use decreases due to positive impacts on the aggregated renewables for all regions, with the largest decrease for North America and Europe, and mainly caused by increased bioenergy use. Under the SSP2-RCP2.6, a reduction in bioenergy use can be expected for some regions (such as the Pacific OECD region) due to low or negative climate impacts on crop yields and higher generation costs. Other robust findings between the IAMs under this mitigation scenario are the expected increase in hydropower use for Rest Asia; an increase in bioenergy use for Europe, Africa and China; and a decrease in solar use for India.

On a global scale, under both scenarios, and considering both IAMs, climate change impacts induce an increase in the primary renewable energy use, with the SSP2-RCP2.6 having a slightly smaller impact (5.2% on average) than the SSP2-RCP6.0 scenario (6% on average). The difference in outcome is smaller than initially expected given the lower impacts on energy potential under the RCP2.6 scenario. When implementing this mitigation scenario in the IAMs, a carbon-pricing strategy is set to favour renewables over fossil fuel sources, which induces a larger increase in renewables use over time. Energy systems with a high share of renewables (e.g. SSP2-RCP2.6 scenario) can have part of their additional (backup) capacity covered by renewables. Therefore, the impacts on the energy system under the SSP2-RCP2.6 scenario have larger sensitivity to changes in energy potential. Also note that the impacts on renewable energy potential could be intensified under the RCP8.5 scenario.

Larger uncertainties were observed for the SSP2-RCP2.6 scenario based on outcome variations between IAM models across the GCMs. There is more variation in impact directions (increase or decrease) between the IAMs outcomes for several source-region combinations under this scenario, especially for the region of the Middle East on bioenergy use and for indirect impacts on fossil energy sources in most regions. Given the uncertainty found across the IAMs, future research would benefit from including more energy models. Furthermore, it should be noted that some energy technologies that could be relevant for the overall assessment remained outside the scope of this study, such as climate impacts on thermal power plants with nuclear and fossil feedstock [15]. Also, note that the IAMs used focus on long-term changes and have a regional scope. Therefore, extreme weather events attributed to climate change were not included in the present analysis, and they could have significant impacts on the energy system. Finally, the patterns of land-use change (LUC) used by the GCM models can vary from those obtained within the IAMs, which can influence the climate impact results; especially for the SSP2-RCP2.6 scenario where more LUC can be expected by the larger deployment of renewables. This could be improved by fully integrating the GCM and the IAM models which is not possible in the context of this research.

Data availability statement

The data that support the findings of this study are available upon reasonable request from the authors.

Acknowledgments

We wish to thank the JPI Climate initiative and participating grant institutes for funding the ISIPedia project. The paper benefitted from funding from the European Research Council under grant ERC-CoG PICASSO (n° 819566).

Code availability

The computer codes used for model comparison of climate impacts on the energy system are available from the corresponding author upon reasonable request.

Conflict of interest

The authors have declared that no competing interests exist.

Appendix A. Methods for power investment

A.1. IMAGE

Here we synthesise the explanation given in [22] for power investment in the electricity module of IMAGE. In this model, the market share of energy technologies is modelled using a multinomial logit function (equation (1)). The LC of technologies, as explained in section 2 of the paper, is used as input data for investment decisions. This LC per technology is calculated for each load band of a RLDC with the implementation of a load factor. A LDC shows the distribution of load over a year (or months) sorted from higher load to lower load, and RLDCs show the remaining load after supplying with variable renewables energies (VRE, such as solar PV and wind).

The load factor for each load-band enables less-capital intensive technologies (such as gas-fired powerplants) to be more attractive for covering the peak loads. Technologies with lower operational costs, such as coal-fired or nuclear power plants, are favoured for covering the baseload of RLDCs. Further, a specific load band with its load factor is assigned for VRE. All technologies (both VRE and non-VRE) compete in this load band based on their LC at the VRE load factor. The capacity to be invested, so-called ordered capacity (equation (1)), is calculated based on the expected capacity needed considering the construction time of the new powerplants. Furthermore, it depends on the estimated future energy demand and retirement time of power plants. Investment in the other renewables category (mainly geothermal) is exogenously determined.

$$\begin{aligned}&\text{IMAGE} - \text{Investment}_{\text{tech}}\\&\quad = \text{ordered capacity}\\&\quad \times \sum_{\text{NB}=1}^{\text{NLB}} \frac{\text{capacity}_{\text{LB}} \times e^{-\lambda\,\text{LC}_{\text{tech}}}}{\sum_{\text{NB}=1}^{\text{NLB}} \text{capacity}_{\text{LB}} \sum_{\text{tech}=1}^{\text{ntech}} e^{-\lambda\,\text{LC}_{\text{tech}}}}\end{aligned} \tag{1}$$

where:
tech = technology
ntech = total number of technologies
LB = load band
NLB = total number of load bands
λ = logit parameter
LCtech = levelized cost of a technology

A.2. GCAM

The information given here provides an overview of the power-sector investment method in GCAM, as explained in [6, 14]. The market share of energy technologies is modelled using a logit function (equation (2)), in which the share of a specific technology is determined by the 'share weight' parameter and the 'logit' exponent. Logit exponents are exogenous parameters that control the degree to which cost determines share, whereas share weights are calculated using historical data to warrant that GCAM reproduces historical data (although they can be modified in future periods depending on the scenario) [14]. The logit function assigns larger shares to lower-cost technologies, although the more expensive options also receive some market share. Note that hydropower is left out of economic competition. The default GCAM projections of hydropower generation are predetermined quantities (derived from the economic and technical potentials estimated by the International Hydropower Association) for each GCAM region and time-step, which are exogenously specified at the start of a simulation [9]. For the present study, we used the hydropower potential input data to compute relative changes (%) in future hydropower potential relative to the historical period (1971–2000). These relative changes were superimposed onto the default projected hydropower production pathway for all GCAM regions. Also, note that GCAM does not implement cost curves for bioenergy. The biomass potentials computed in this study are used to place constraints on total biomass production in each GCAM region. I.e. the magnitudes of total regional biomass produced as calculated by GCAM cannot surpass the limits imposed by the energy potentials computed here.

$$S_{T,t} = \frac{\alpha_{T,t} p_{T,t}^{\gamma}}{\sum_{T=1}^{N} \alpha_{T,t} p_{T,t}^{\gamma}} \tag{2}$$

where:
$p_{T,t}$ = the levelized cost of the technology T in time period t
γ = exogenous input shape parameter called 'logit exponent'
$\alpha_{T,t}$ = calibration parameters called 'share weights'.

Appendix B. Overview of technical and economic assumptions

The tables 2 and 3 provide an overview of the technical and economic assumptions for the different renewable energy technologies for IMAGE and GCAM. The electric power-sector technology assumptions given are capital cost (CAPEX, \$ kW^{-1} (2017)), learning rate, technical and economic lifetimes (years), and fixed and variable operation and maintenance cost (\$ kW^{-1} (2005)).

Note the following: CAPEX cost and technology learning rate in IMAGE change depending on the scenario implemented (here, they are given for the SSP2-RCP60 scenario). Furthermore, the learning rate of technologies is only implemented by IMAGE. However, in GCAM, technology efficiencies improve over time. The CAPEX cost data used in GCAM is for the years 2015 and 2020 instead of 2017. Then,

Table 2. Technical and economic assumptions for IMAGE and GCAM.

						OPEX ($ kW^{-1})			
		Learning rate		Technical lifetime (years)		O&M fixed		O&M variable	
Region	Technology	IMAGE	GCAM	IMAGE	GCAM	IMAGE	GCAM	IMAGE	GCAM
World	Utility-scale PV	0.2	—	25	30	17	36	0	0
	Rooftop PV	0.2	—	25	30	20	54	0	0
	CSP	0.1	—	25	30	66	50	4	0
	Wind onshore	0.07	—	25	30	51	45	0	0
	Wind offshore	0.15	—	25	—	134	—	0	—
	Hydro	0.01	—	80	—	40	—	0	—
	Conv. bio-energy	0.05	—	40	60	107	86	5	9
	CombCycle bio-energy	0.02	—	40	60	127	127	7	14

Table 3. Capital cost assumptions for IMAGE and GCAM for selected regions.

		CAPEX ($ kW^{-1})							
		2017		2030		2040		2050	
Region	Technology	IMAGE	GCAM	IMAGE	GCAM	IMAGE	GCAM	IMAGE	GCAM
USA	Utility-scale PV	1458	2042	945	1858	754	1754	696	1678
	Rooftop PV	3264	5142	1416	4677	867	4413	811	4222
	CSP	6670	5124	5771	4215	5260	3814	5137	3576
	Wind onshore	1602	2189	1199	1988	1046	1880	1026	1797
	Wind offshore	2178	—	1637	—	1421	—	1362	—
	Hydro	2789	—	2786	—	2784	—	2783	—
	Conv. bio-energy	2678	4444	2645	4316	2637	4222	2633	4139
	Combined Cycle bio-energy	3141	6566	3093	5968	3074	5636	3059	5387
Western Europe or EU-15	Utility-scale PV	1238	2042	907	1858	757	1754	698	1754
	Rooftop PV	1571	5142	1065	4677	870	4413	813	4413
	CSP	5775	5124	5560	4215	5258	3814	5135	3814
	Wind onshore	1785	2189	1246	1988	1047	1880	1026	1880
	Wind offshore	2360	—	1684	—	1421	—	1363	—
	Hydro	2599	—	2786	—	2784	—	2783	—
	Conv. bio-energy	2465	4444	2543	4316	2538	4222	2533	4222
	Combined Cycle bio-energy	2928	6566	2991	5968	2974	5636	2959	5636
India	Utility-scale PV	1086	2042	877	1858	757	1754	698	1754
	Rooftop PV	1191	5142	986	4677	871	4413	813	4413
	CSP	5751	5124	5244	4215	4921	3814	4874	3814
	Wind onshore	1108	2189	1072	1988	1047	1880	1026	1880
	Wind offshore	1684	—	1510	—	1422	—	1363	—
	Hydro	1973	—	2063	—	2172	—	2307	—
	Conv. bio-energy	2169	4444	2190	4316	2245	4222	2316	4222
	Combined Cycle bio-energy	2632	6566	2639	5968	2681	5636	2742	5636
China+	Utility-scale PV	1084	2042	875	1858	756	1754	697	1754
	Rooftop PV	1311	5142	1010	4677	870	4413	812	4413
	CSP	5235	5124	5222	4215	5099	3814	5085	3814
	Wind onshore	1218	2189	1099	1988	1046	1880	1026	1880
	Wind offshore	1793	—	1536	—	1421	—	1363	—
	Hydro	2142	—	2321	—	2498	—	2700	—
	Conv. bio-energy	1852	4444	1932	4316	2025	4222	2134	4222
	Combined Cycle bio-energy	2315	6566	2380	5968	2462	5636	2559	5636

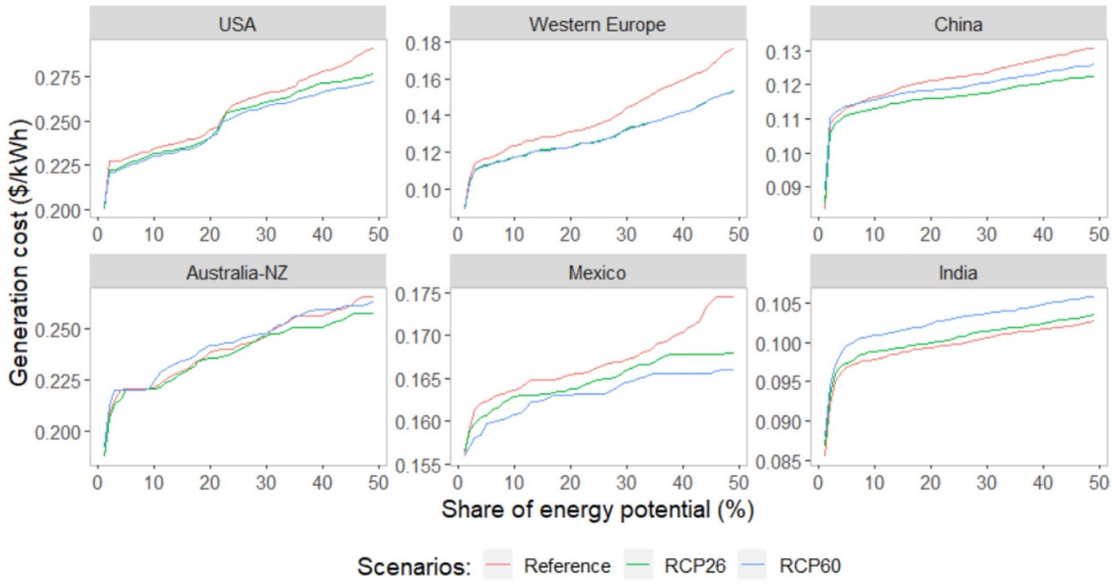

Figure 6. PV rooftop cost–supply curves input data used for selected regions using MIROC5 climate data for the historical reference scenario (1971–2000) and future projections (2071–2100) for the RCP26 and the RCP60 scenarios.

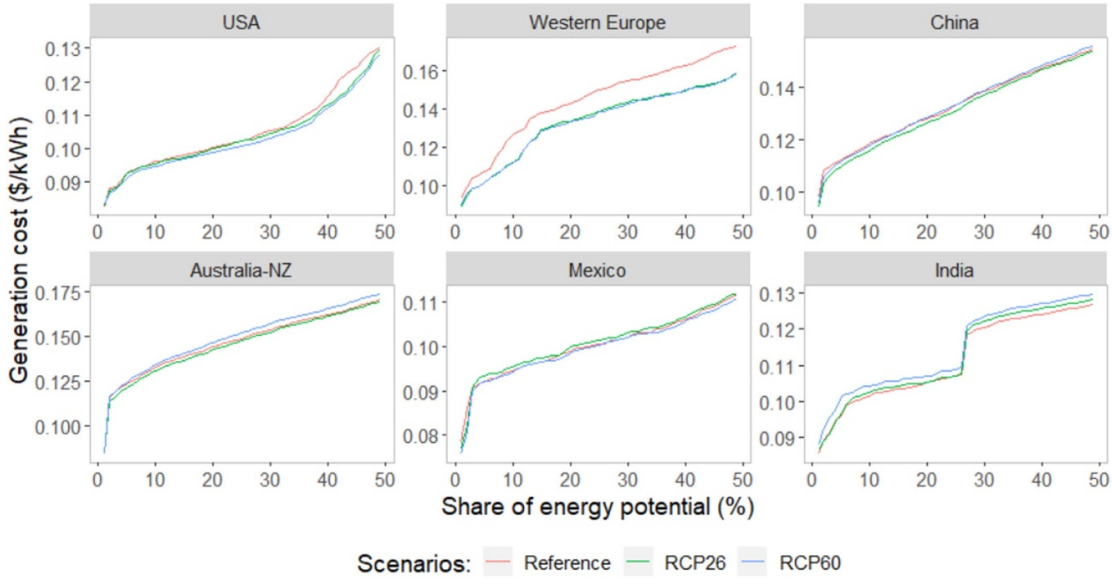

Figure 7. PV utility cost–supply curves input data used for selected regions using MIROC5 climate data for the historical reference scenario (1971–2000) and future projections (2071–2100) for the RCP26 and the RCP60 scenarios.

for this table, the GCAM CAPEX value for 2017 is a linear interpolation between 2015 and 2020 values. In GCAM, O&M fixed varies by year; below, it is given for 2010 (the last calibrated year). The assumptions for hydropower in GCAM are not given because hydropower projections in this model are exogenously determined (hence, independent of economic competition as mentioned in appendix A). Finally, GCAM v5.2 does not include wind offshore.

Appendix C. Cost–supply curves

In this section, the input data of cost–supply curves for selected regions are provided in figures 6 to 13. The climate model MIROC5 was selected for illustration purposes and for maintaining comparability between the energy sources. Note that in GCAM, the cost supply curves for wind and solar sources are the only ones implemented, while in IMAGE, all cost supply curves are used.

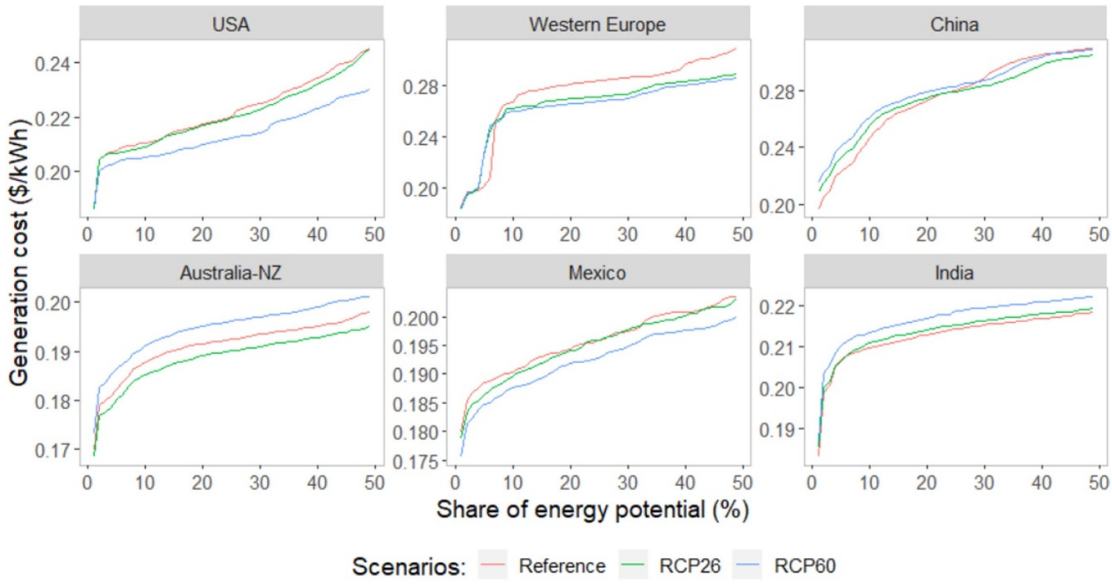

Figure 8. CSP cost–supply curves input data used for selected regions using MIROC5 climate data for the historical reference scenario (1971–2000) and future projections (2071–2100) for the RCP26 and the RCP60 scenarios.

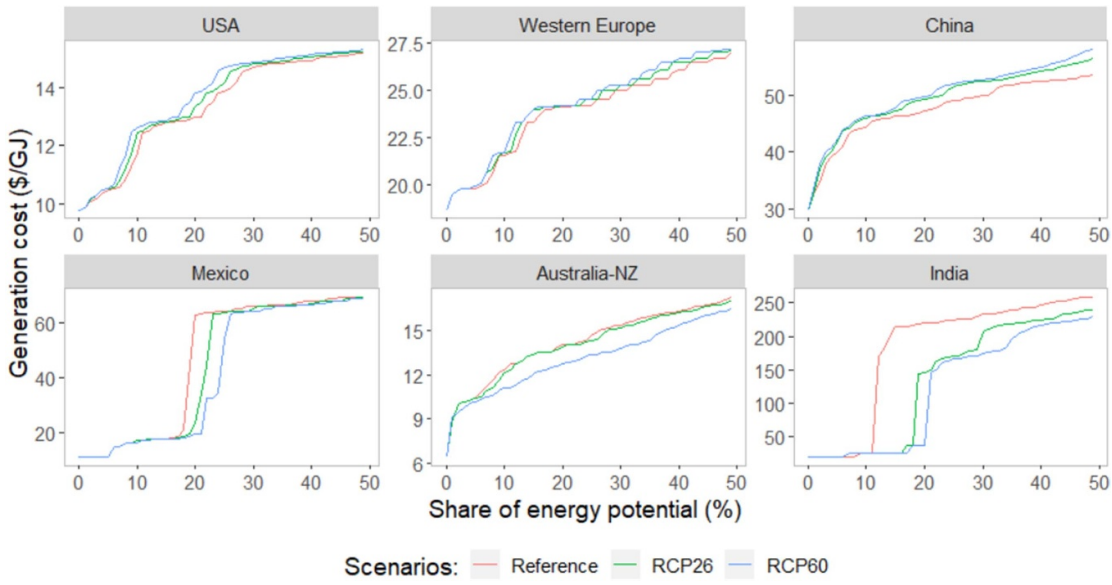

Figure 9. Biomass 1st generation cost–supply curves input data used for selected regions using MIROC5 climate data for the historical reference scenario (1971–2000) and future projections (2071–2100) for the RCP26 and the RCP60 scenarios.

Appendix D. Further climate impact analysis

D.1. Climate change impacts for the period 2031-2070

Figure 14 shows the climate change impacts for the period 2031–2070 under the SSP2-RCP6.0 scenario. For this period, large impacts are also projected for bioenergy use from the two IAMs (world average of 8% ± 18%) due to the consideration of CO_2 fertilisation. The largest variation between the IAMs response to climate impacts across the GCMs data is for solar energy, especially for North America, the Reforming Economic region and Latin America. There, GCAM shows a decrease in solar use for most of the regions, while IMAGE response shows the opposite. Further, for hydropower use, there is also a large variation between the IAMs results for the region of Reforming Economies due to differences in indirect impacts related to system compensation from the increased use of other renewables.

Overall, the IAMs show an increase in renewables use in all regions, but as expected, the impacts are lower than for the period 2071–2100. The largest impact can be expected in North America according to IMAGE results by an increase in bioenergy use,

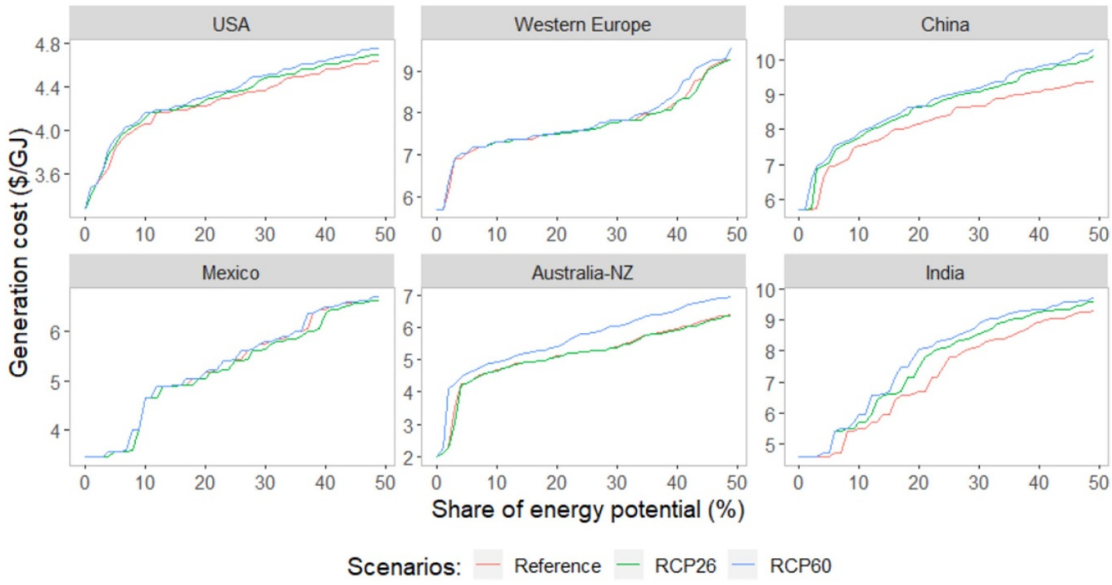

Figure 10. Biomass 2nd generation cost–supply curves input data used for selected regions using MIROC5 climate data for the historical reference scenario (1971–2000) and future projections (2071–2100) for the RCP26 and the RCP60 scenarios.

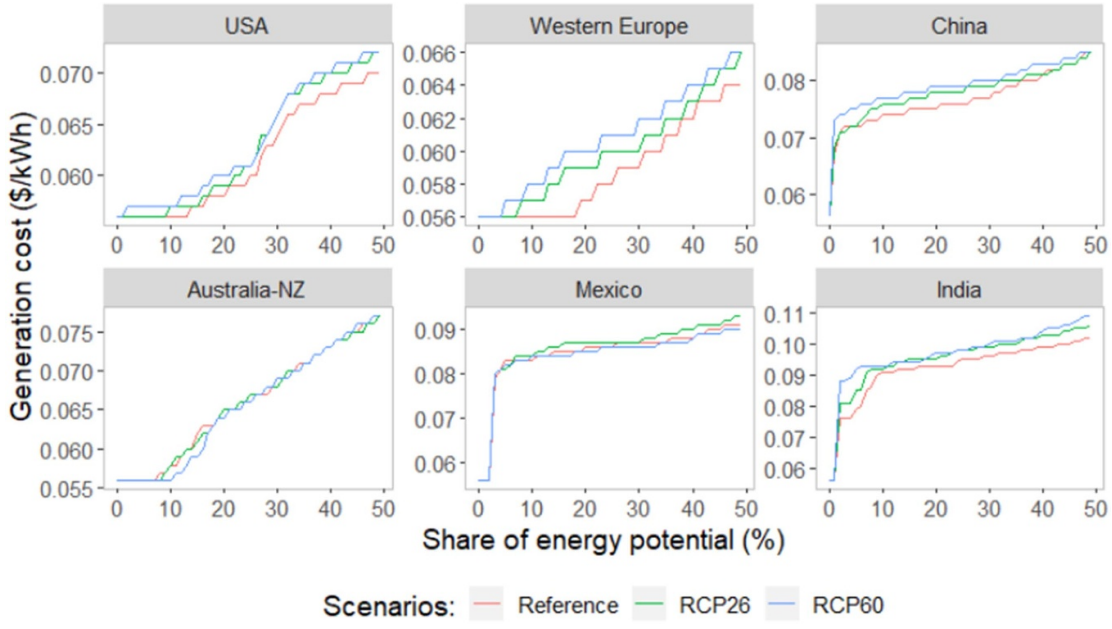

Figure 11. Wind offshore cost–supply curves input data used for selected regions using MIROC5 climate data for the historical reference scenario (1971–2000) and future projections (2071–2100) for the RCP26 and the RCP60 scenarios.

and in the Reforming Economic region according to GCAM results by an increase in hydropower use. Furthermore, the Pacific-OECD region has the largest reduction in the use of wind and hydropower across the IAMs due to a reduction in the energy potentials by climate impacts. Concerning fossil sources, globally and for all regions, a slight reduction (between 0% and 4%) in the use of fossil energy is expected as a result of climate impacts on renewable energy, according to results from both IAMs. Only for the Latin America region, and according to results from one GCM run (GFDL-ESM-2M), a minimal increase in fossil energy use could be expected. In contrast, the largest decrease in fossil use can be expected for North America, Pacific OECD and Europe regions.

Figure 15 shows climate change impacts under the SSP2-RCP2.6 scenario for this period. The average world impacts on the use of renewables are similar to the SSP2-RCP6.0. Biomass and wind sources are the most impacted by climate change. The largest impact is expected for China from an increased use of wind and biomass energies. Europe also has a large

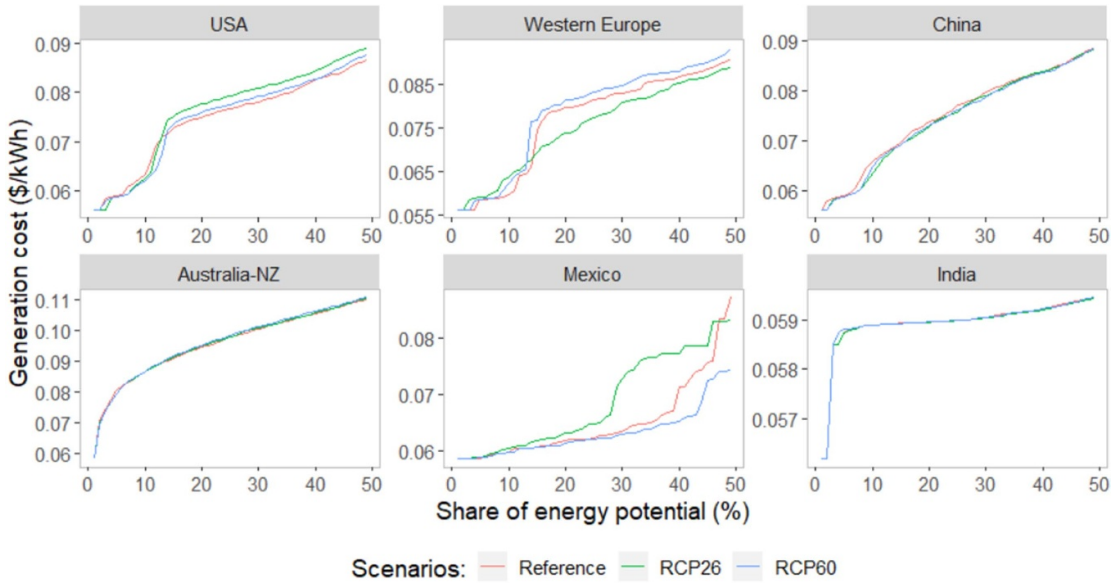

Figure 12. Wind onshore cost–supply curves input data used for selected regions using MIROC5 climate data for the historical reference scenario (1971–2000) and future projections (2071–2100) for the RCP26 and the RCP60 scenarios.

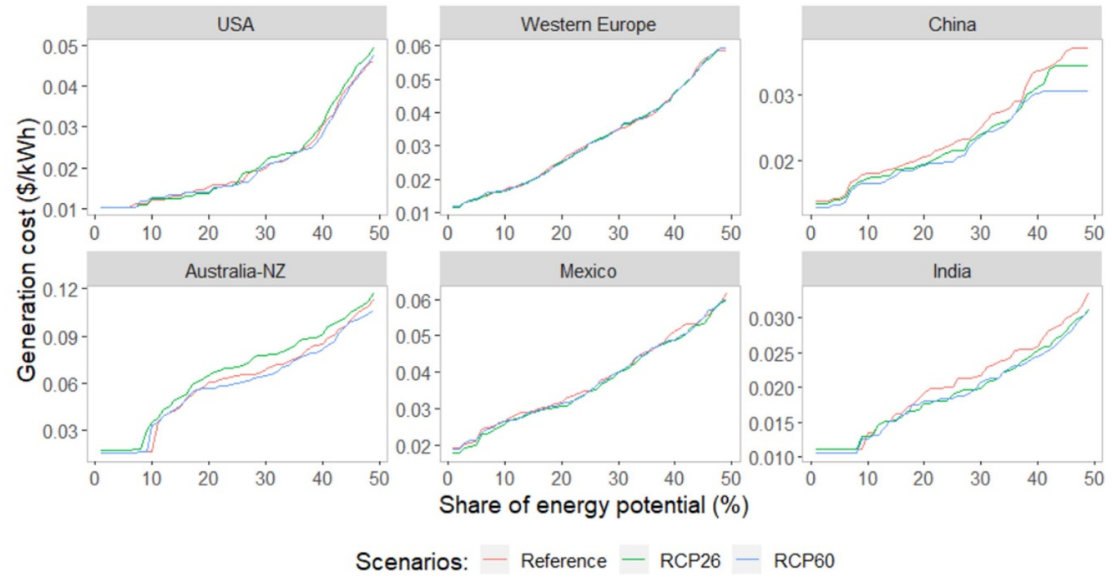

Figure 13. Hydropower cost–supply curves input data used for selected regions using MIROC5 climate data for the historical reference scenario (1971–2000) and future projections (2071–2100) for the RCP26 and the RCP60 scenarios.

impact due to the increased biomass use. The Pacific OECD region is the only one with a decreased use of mean renewables due to a decrease in biomass and wind use.

Under this scenario and period, also significant variation between the IAMs response to climate impacts is found for solar energy use. Especially for the regions of Reforming Economies, Pacific OECD, Middle East and North America, where the IAMs do not agree on the direction in response to climate impact across at least three GCMs. Furthermore, variations between the IAMs response were also found for several cases for bioenergy use. Especially in the Middle East, Latin America and the Reforming Economies region. However, a consistent increase in bioenergy use by climate impacts (across IAMs and most GCMs) is expected for Europe, China and Africa. Other consistent impacts by climate change are the increase of hydropower use in Europe, India and the Rest Asia region; and the increase in wind energy use in Latin America and Rest Asia region from IAMs results across three GCMs.

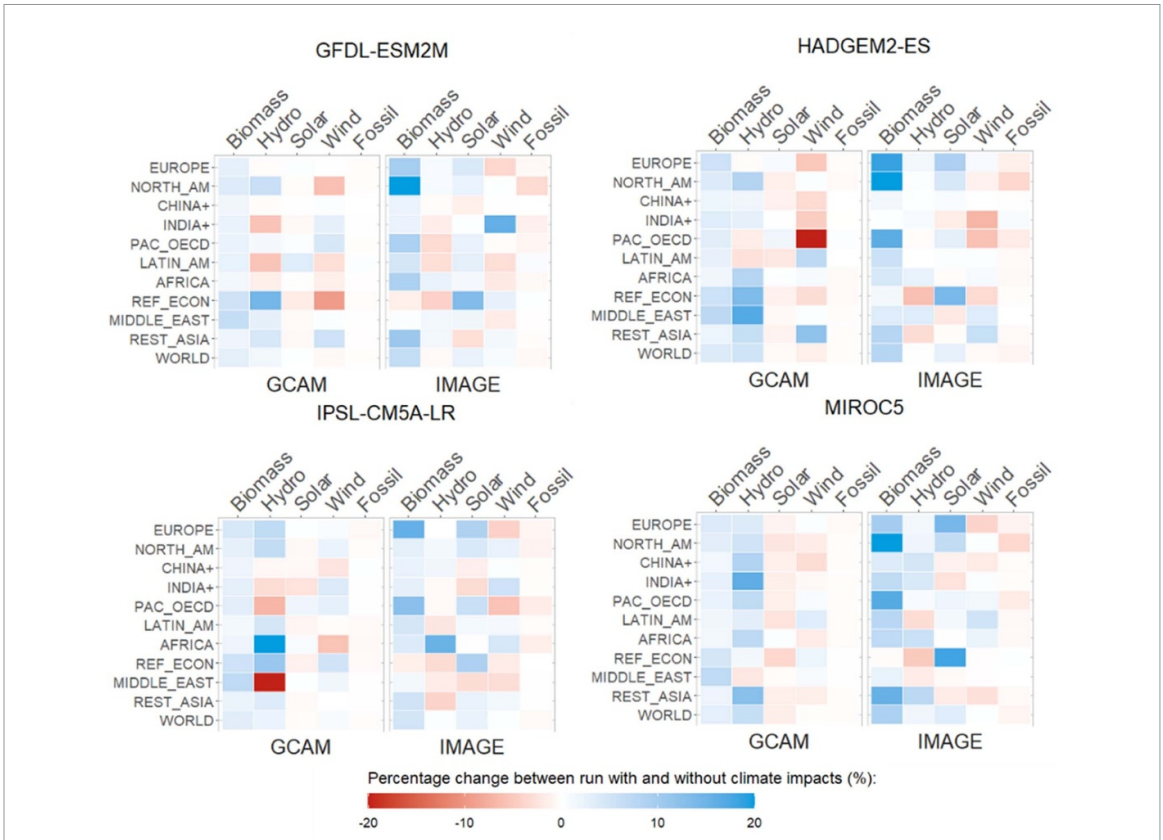

Figure 14. Climate impacts combined effect on primary energy generation under the SSP2-RCP6.0 scenario for the period 2031–2070. Impacts are compared between IMAGE and GCAM for each GCM (top left: GFDL-ESM2M, top right: HADGEM2-ES, bottom left: IPSL-CM5A-LR, and bottom right: MIROC5). Blue tones represent positive impacts and red tones negative impacts by climate change.

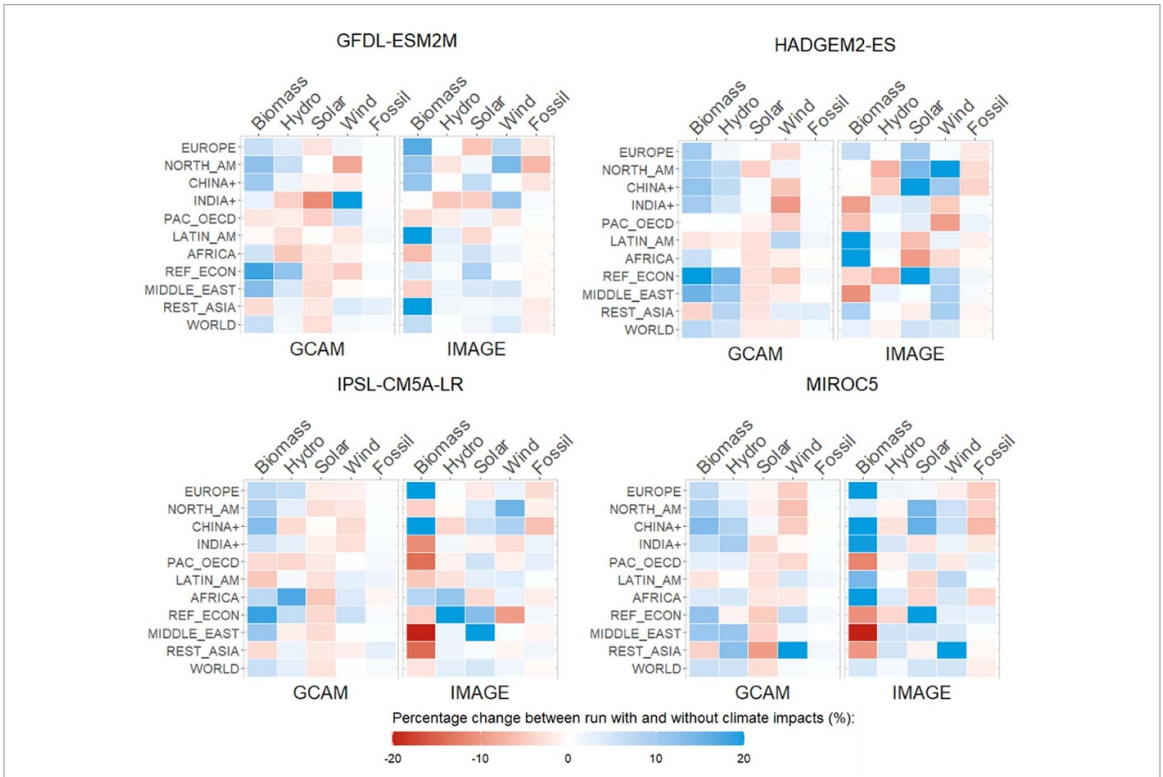

Figure 15. Climate impacts combined effect on primary energy generation under the SSP2-RCP2.6 scenario for the period 2031–2070. Impacts are compared between IMAGE and GCAM for each GCM (top left: GFDL-ESM2M, top right: HADGEM2-ES, bottom left: IPSL-CM5A-LR, and bottom right: MIROC5). Blue tones represent positive impacts and red tones negative impacts by climate change.

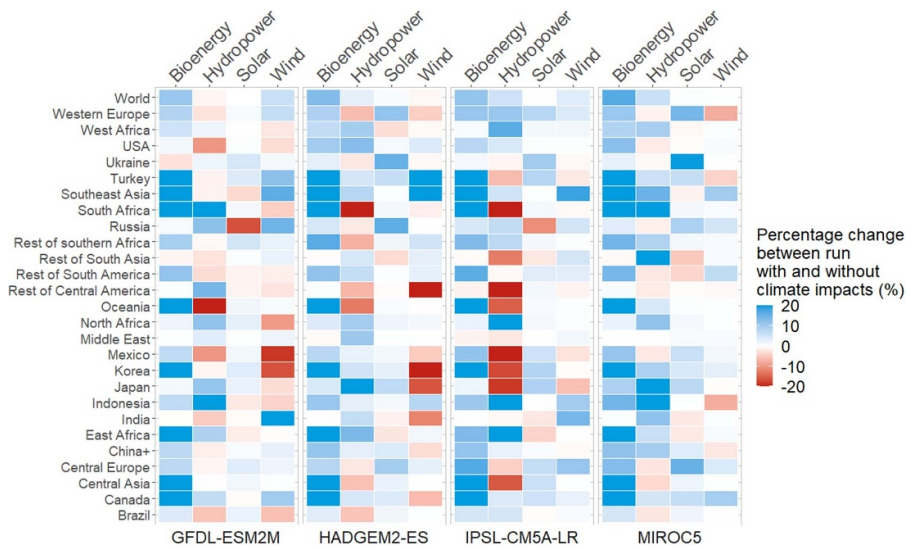

Figure 16. The direct effect of climate impacts on cumulative primary energy in SSP2-RCP60 (2070–2100) analysed with IMAGE. The graphs correspond to the percentage change of renewable use with and without climate impact for the four GCMs (GFDL-ESM2M, HADGEM2-ES, IPSL-CM5A-LR, and MIROC5). Blue tones represent positive impacts and red tones negative impacts by climate change.

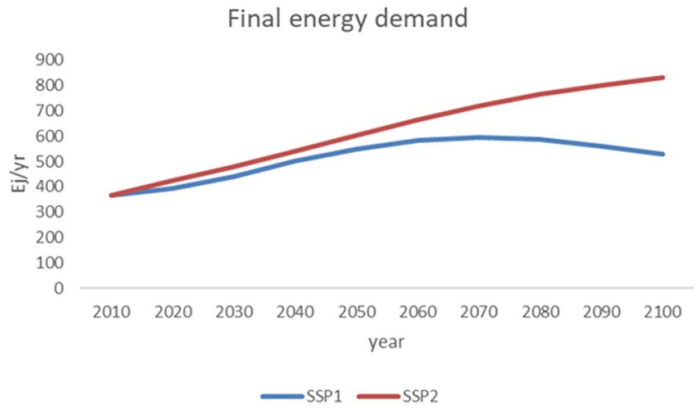

Figure 17. Total final energy demand for the world under the SSP1 and SSP2 baseline scenarios.

D.2. Direct impacts on renewables

Figure 16 shows direct climate impacts on all renewables using IMAGE model under the SSP2-RCP60 scenario. For the comparison exercise between IMAGE and GCAM, we selected the sources with the largest impact on their energy potential, biomass with positive impact and wind energy with negative impact.

D.3. SSP1 scenario

To analyse the effect of climate impacts at different demand levels, we also analysed the impacts under the SSP1-RCP60 scenario. The RCP6.0 cost supply curves were implemented in the IMAGE model running the SSP1 baseline scenario which has a lower demand level than the SSP2 baseline scenario (figure 17). The results show (figure 18) that impacts under the SSP1-RCP60 denote very similar magnitude to the SSP2-RCP60 runs for most regions.

D.4. Calculated standard deviations

Tables 4 and 5 show the standard deviation of climate impacts on the energy under both scenarios considered. Under the reference scenario (SSP2-RCP60), the dispersion is larger for bioenergy for most regions. This can be related to considerably larger impacts in the results from IMAGE than GCAM as shown in figure 2 of the main text.

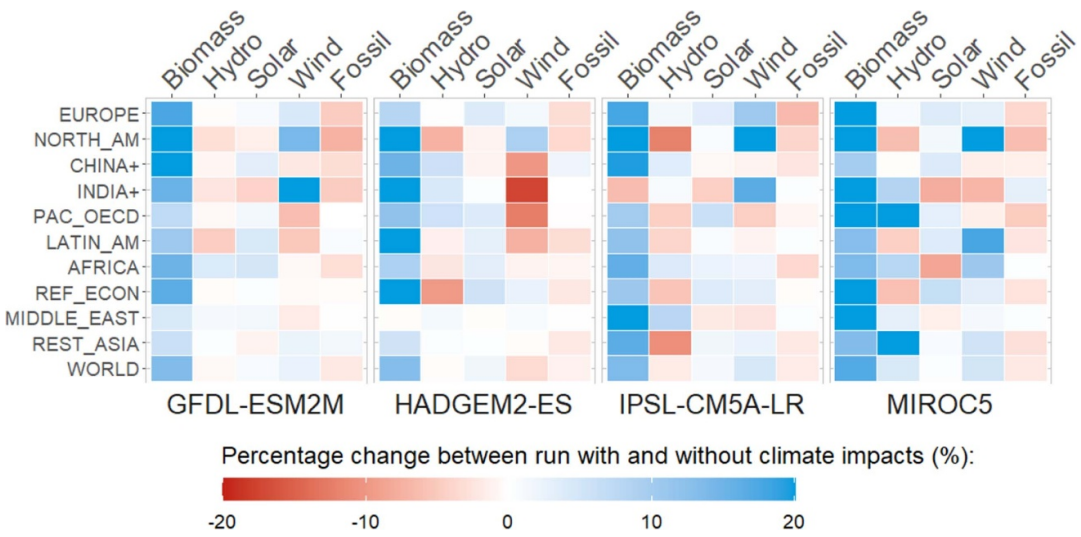

Figure 18. Changes in primary energy use under the SSP1-RCP6.0 scenario between the runs with and without climate change impacts for the period 2071–2100 for each GCM. Blue tones represent positive impacts and red tones negative impacts by climate change.

Table 4. Standard deviation of the climate impacts on the energy system under the SSP2-RCP6.0 for the period 2071–2100.

Region	Biomass	Hydro	Solar	Wind
AFRICA	38.55	13.65	1.73	4.03
CHINA+	4.46	6.11	2.16	2.92
EUROPE	23.96	4.44	5.00	5.72
INDIA+	2.69	10.64	2.74	17.29
LATIN_AM	2.45	5.32	2.33	5.81
MIDDLE_EAST	5.55	15.50	2.46	4.79
NORTH_AM	64.50	4.34	4.09	6.43
PAC_OECD	15.21	12.67	2.86	8.01
REF_ECON	4.56	9.06	7.68	10.43
REST_ASIA	9.76	6.84	2.88	14.80

Table 5. Standard deviation of the climate impacts on the energy system under the SSP2-RCP2.6 for the period 2071–2100.

Region	Biomass	Hydro	Solar	Wind
AFRICA	6.76	8.90	3.76	3.79
CHINA+	17.92	6.27	4.12	5.31
EUROPE	12.51	4.05	8.54	6.56
INDIA+	9.38	4.83	1.77	10.14
LATIN_AM	17.09	4.05	3.72	10.13
MIDDLE_EAST	18.74	6.68	3.46	7.00
NORTH_AM	13.60	3.69	99.12	11.81
PAC_OECD	5.31	13.73	5.31	6.24
REF_ECON	22.68	7.28	29.33	10.01
REST_ASIA	7.20	5.88	6.55	87.61

Appendix E. Primary energy projections from IAMs

Primary energy use projections from renewables and fossil sources under the SSP2 reference scenario with climate change effect (SSP2-RCP6.0-CI) is illustrated in figure 19. For 2010, primary use values are based on historical climate data, and then they are not influenced by climate change. For the year 2050, the values have a higher variation between the IAMs. IMAGE has lower use estimation for this year from fossil sources; however, the share of renewable energy sources is larger, especially from wind and solar sources. For 2100, energy use from wind and solar sources continues to grow faster in IMAGE model. Note that nuclear energy and other sources, such as residues feedstock for biomass, traditional biomass, geothermal, tidal and wave energy, are not included in these figures. Figure 20 shows the primary energy projections for the SSP2 mitigation scenario (SSP2-RCP2.6-CI), considering the climate change effect.

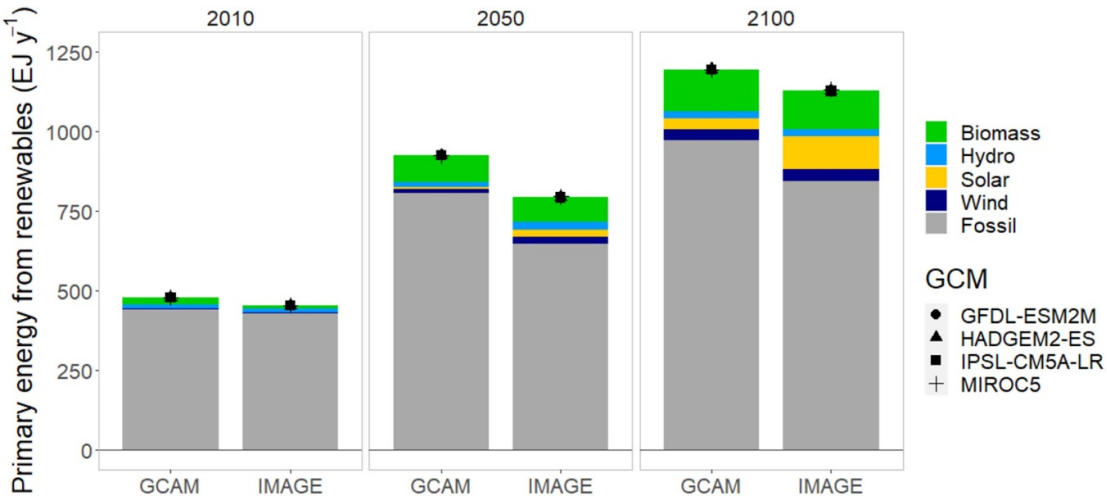

Figure 19. Global primary energy use per energy carrier with climate impact for the SSP2 baseline scenario (SSP2-RCP6.0-CI).

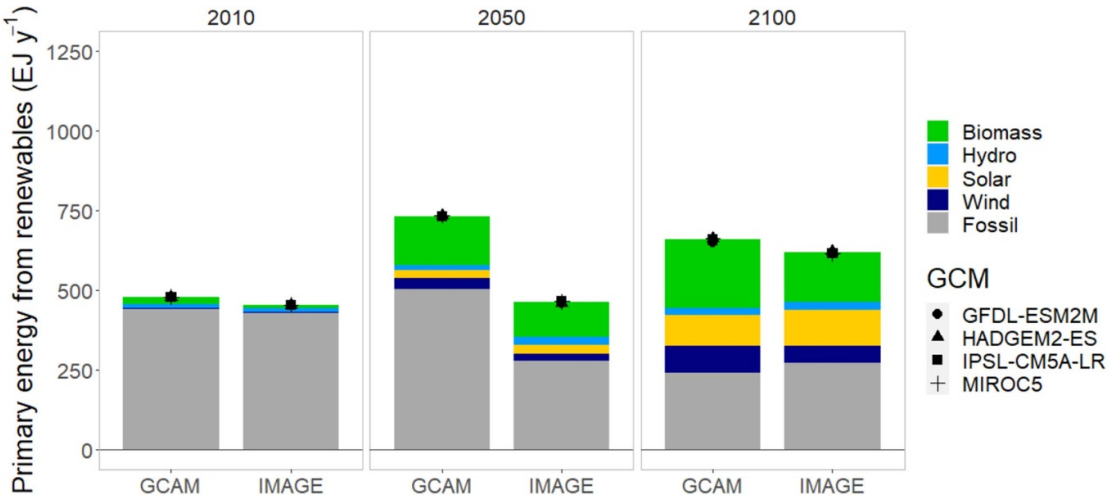

Figure 20. Global primary energy use per energy carrier with climate impact for the SSP2 mitigation scenario (SSP2-RCP2.6-CI).

Appendix F. Super regions

The region division implemented in this research corresponds to a 'super region' division commonly used for IAMs model comparison. Each region is explained below.

- AFRICA: countries of Sub-Saharan Africa.
- CHINA+: countries of centrally-planned Asia, primarily China.
- EUROPE: countries of Eastern and Western Europe (i.e. the EU27).
- INDIA+: countries of South Asia; primarily India.
- LATIN_AM: countries of Latin America and the Caribbean.
- MIDDLE_EAST: countries of the Middle East.
- NORTH_AM: countries of North America; primarily the USA and Canada.
- PAC_OECD: countries of the Pacific OECD (Organization for Economic Co-operation and Development). They are Japan, Australia, and New Zealand.
- REF_ECON: countries from the Reforming Economies of Eastern Europe and the Former Soviet Union.
- REST_ASIA: Asian countries excluding China and India.

Appendix G. Scenarios data

The figures 21 and 22 illustrate main scenario data used for this research.

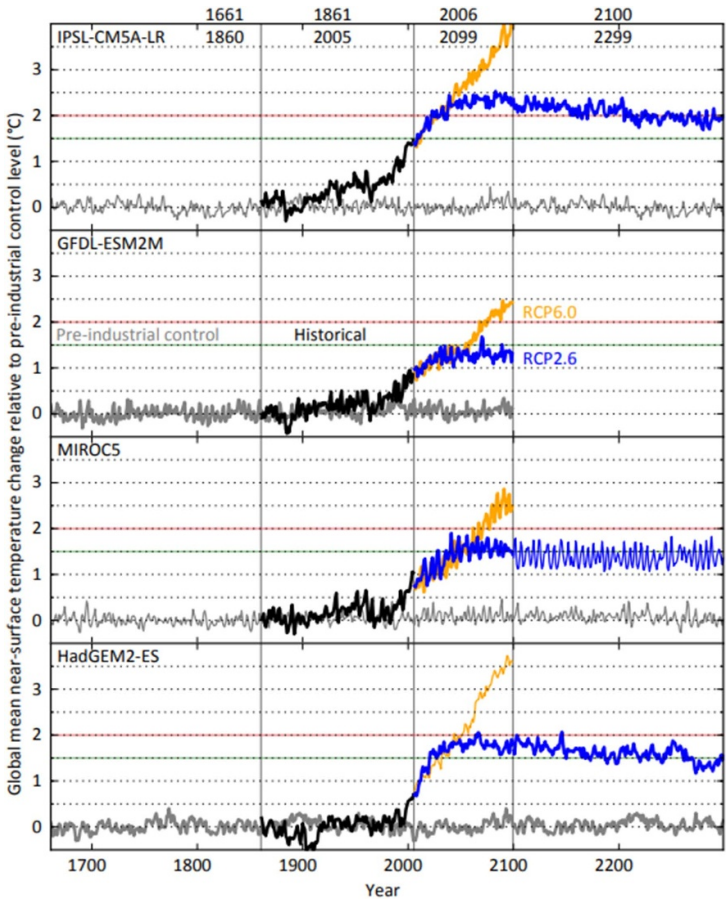

Figure 21. Time series of annual global mean near-surface temperature change relative to pre-industrial levels (1661–1860) from the different GCMs modelled data used in this research (IPSL-CM5A-LR, GFDL-ESM2M, MIROC5, and HADGEM2-ES). The colour coding represents the different scenarios for the periods indicated at the top. Grey: the pre-industrial control scenario, black: historical values, blue: the RCP2.6 scenario, and yellow: the RCP6.0 scenario. Reproduced from Frieler et al [7]. CC BY 3.0.

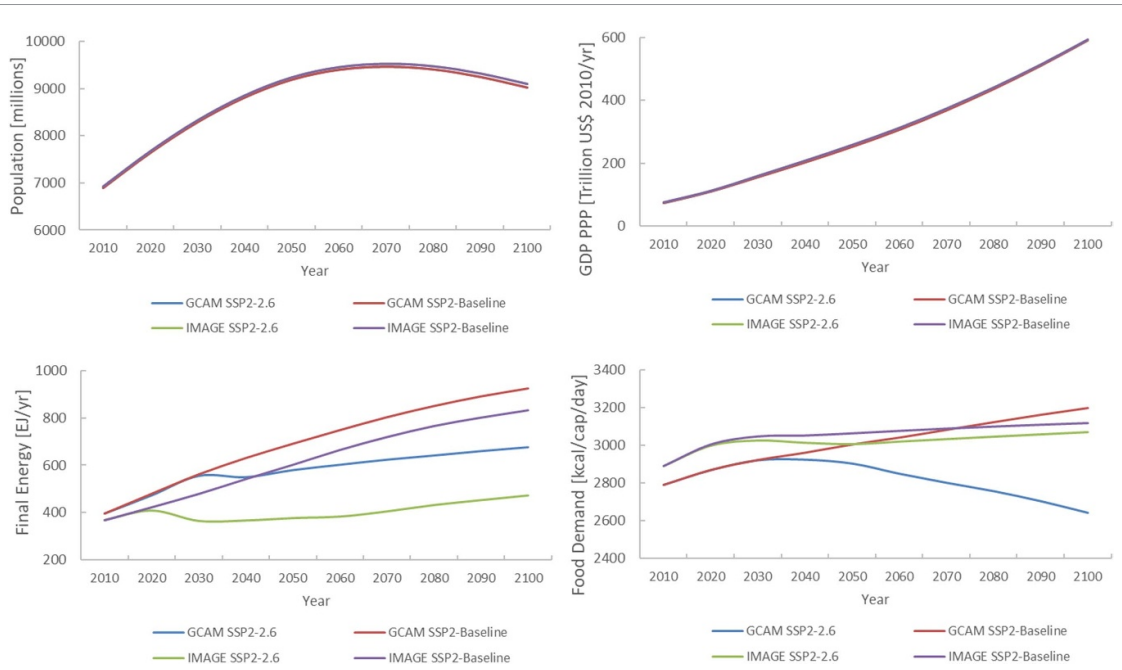

Figure 22. IMAGE and GCAM SSP assumptions for the world on population, economic development, final energy demand and food demand. (Data obtained from Huppmann et al, IAMC 1.5 °C scenario explorer and data hosted by IIASA, url: data.ene.iiasa.acat/iamc-1.5c-explorer).

ORCID iDs

Victhalia Zapata https://orcid.org/0000-0001-8274-0173
Silvia R Santos da Silva https://orcid.org/0000-0002-6493-1475

References

[1] IEA Global energy & CO_2 status report 2019 (available at: www.iea.org/reports/global-energy-co2-status-report-2019/emissions) (Accessed 22 June 2020)
[2] Yalew S G *et al* 2020 Impacts of climate change on energy systems in global and regional scenarios *Nat. Energy* **5** 794–802
[3] Cronin J, Anandarajah G and Dessens O 2018 Climate change impacts on the energy system: a review of trends and gaps *Clim. Change* **151** 79–93
[4] Solaun K and Cerdá E 2019 Climate change impacts on renewable energy generation. A review of quantitative projections *Renew. Sustain. Energy Rev.* **116** 109415
[5] Gernaat D E H J, de Boer H S, Daioglou V, Yalew S G, Müller C and van Vuuren D P 2021 Climate change impacts on renewable energy supply *Nat. Clim. Change* **11** 119–25
[6] Santos da Silva S R *et al* 2021 Power sector investment implications of climate impacts on renewable resources in Latin America and the Caribbean *Nat. Commun.* **12** 1–12
[7] Frieler K *et al* Assessing the impacts of 1.5 °C global warming-simulation protocol of the inter-sectoral impact model intercomparison project (ISIMIP-2b) *Geosci. Model Dev.* **10** 4321–45
[8] Stehfest Eof Global Environmental Change with IMAGE 3.0 2014 Model description and policy applications. Netherlands Environmental Assessment Agency (PBL) p 370 (available at: www.pbl.nl/en/publications/integrated-assessment-of-global-environmental-change-with-IMAGE-3.0 (Accessed October 2020))
[9] Joint Global Change Research Institute (JGCRI) GCAM v5.2 documentation (available at: https://jgcri.github.io/gcam-doc/v5.2/overview.html) (Accessed 6 July 2020)
[10] Gernaat D E H J, Bogaart P W, Van Vuuren D P, Biemans H and Niessink R 2017 High-resolution assessment of global technical and economic hydropower potential *Nat. Energy* **2** 821–8
[11] Daioglou V, Doelman J C, Wicke B, Faaij A and van Vuuren D P 2019 Integrated assessment of biomass supply and demand in climate change mitigation scenarios *Glob. Environ. Change* **54** 88–101
[12] Gernaat D E H J, De Boer H S *et al* 2020 The role of residential rooftop photovoltaic in long-term energy and climate scenarios *Appl. Energy* **279** 115705
[13] Netherlands Environmental Assessment Agency (PBL) IMAGE 3.2 documentation (available at: https://models.pbl.nl/image/index.php/Welcome_to_IMAGE_3.2_Documentation) (Accessed 27 October 2020)
[14] Calvin K *et al* 2019 GCAM v5.1: representing the linkages between energy, water, land, climate, and economic systems *Geosci. Model Dev.* **12** 677–98
[15] Van Vliet M T H, Wiberg D, Leduc S and Riahi K 2016 Power-generation system vulnerability and adaptation to changes in climate and water resources *Nat. Clim. Change* **6** 375–80
[16] O'Neill B C *et al* 2014 A new scenario framework for climate change research: the concept of shared socioeconomic pathways *Clim. Change* **122** 387–400
[17] Riahi K *et al* 2017 The shared socioeconomic pathways and their energy, land use, and greenhouse gas emissions implications: an overview *Glob. Environ. Change* **42** 153–68
[18] Rosenzweig C *et al* 2014 Assessing agricultural risks of climate change in the 21st century in a global gridded crop model intercomparison *Proc. Natl Acad. Sci. USA* **111** 3268–73
[19] IAMC wiki The common integrated assessment model (IAM) documentation (available at: www.iamcdocumentation.eu/index.php/IAMC_wiki) (Accessed 27 October 2020)
[20] IEA 2020 World energy balances—statistics report (available at: www.iea.org/reports/world-energy-balances-overview)
[21] Krey V *et al* 2019 Looking under the hood: a comparison of techno-economic assumptions across national and global integrated assessment models *Energy* **172** 1254–67 (available at: www.sciencedirect.com/science/article/pii/S0360544218325039)
[22] de Boer H S, van Vuuren D *et al* 2017 Representation of variable renewable energy sources in TIMER, an aggregated energy system simulation model *Energy Econ.* **1** 600–11